

Nanostructured electrochemical DNA biosensors for detection of the effect of berberine on DNA from cancer cells

Renáta Ovádeková · Soňa Jantová · Silvia Letašiová ·
Ivan Štepánek · Ján Labuda

Received: 17 July 2006 / Revised: 31 August 2006 / Accepted: 4 September 2006 / Published online: 20 October 2006
© Springer-Verlag 2006

Abstract Multi walled carbon nanotubes (MWNT) in dimethylformamide (DMF) or aqueous sodium dodecyl sulfate (SDS) solution, colloidal gold nanoparticles (GNP) in phosphate buffer solution (PBS), and a GNP–MWNT mixture in aqueous SDS solution have been investigated for chemical modification of a screen-printed carbon electrode used as the signal transducer of a dsDNA-based biosensor. Differential pulse voltammetry of the DNA redox marker $\text{Co}[(\text{phen})_3]^{3+}$ and the guanine moiety anodic oxidation and cyclic voltammetry with $\text{K}_3[\text{Fe}(\text{CN})_6]$ as indicator revealed substantial enhancement of the response of the biosensor, particularly when MWNT in SDS solution was used. The biosensor was used in testing of berberine, an isoquinoline plant alkaloid with significant antimicrobial and anticancer activity. Berberine had a very strong, concentration-dependent, effect on the structural stability of DNA from the human cancer cells (U937 cells) whereas non-cancer cells were changed only when berberine concentrations were relatively high 75 and 50 $\mu\text{g mL}^{-1}$.

Keywords DNA-biosensors · Multi walled carbon nanotubes · Gold nanoparticles · DNA from cancer cells · Berberine

Introduction

Modern trends in the development of biosensors, including those based on DNA, use a complex and sophisticated sensor arrangement utilizing bioactivation and the application of (electro)catalytic elements and elements of nanotechnology. Nanoobjects such as nanoparticles of metals, semiconductors, and oxides, and nanostructures such as nanotubes and nanowires could substantially improve the sensitivity of electrochemical sensors and biosensors [1]. Nanostructured materials have been successfully used for detection of DNA damage and DNA immobilization [2].

The unique properties, for example high electrical conductivity, mechanical strength and chemical stability, of multi-walled carbon nanotubes (MWNT) make them extremely suitable for developing electrochemical sensors and biosensors [3]. The chemical and structural properties of MWNT, for example chemical inertness and poor solubility in most solvents, make it difficult to prepare uniform nanotube deposits, however. MWNT are usually temporarily dispersed in solvents, for example dimethylformamide [4], acetone [5], or nafione [6]. Pretreatment by wet oxidation in a mixed acid solution has enabled the MWNT to be covalently functionalized by oxygenated groups, for example carboxyl groups [7]. Functionalized and shortened MWNT can also be assembled layer-by-layer on a solid substrate, because of electrostatic interaction between the MWNT and a polyelectrolyte such as chitosan [8].

Colloidal gold nanoparticles (GNP) are a type of nano-material which might play an important role in the construc-

R. Ovádeková (✉) · J. Labuda
Institute of Analytical Chemistry,
Faculty of Chemical and Food Technology,
Slovak University of Technology in Bratislava,
81237 Bratislava, Slovakia
e-mail: renata.ovadekova@stuba.sk

S. Jantová · S. Letašiová
Institute of Biochemistry, Nutrition and Health Protection,
Faculty of Chemical and Food Technology,
Slovak University of Technology in Bratislava,
81237 Bratislava, Slovakia

I. Štepánek
Private Secondary Technical School ELBA,
Smetanova 2,
08001 Prešov, Slovakia

tion of electrochemical DNA biosensors. GNP have very large surface area and good biocompatibility [9]. They also increase the stability of DNA binding on electrode surface.

The interactions of anticancer agents with DNA have been investigated by a variety of techniques and there is a growing interest in the use of electrochemical methods and sensors on this field, particularly for testing of dose-response relationships [2]. Berberine (Fig. 1), an isoquinoline plant alkaloid widely used in traditional Chinese and Ayurvedic medicine, has a broad range of pharmacological and biochemical effects [10], including significant antimicrobial [11] and anticancer [12] activity. Berberine also has anti-inflammatory and antipyretic effects [13], antihypertension and antiarrhythmia action, antibiotic activity, antimotility action, protective effects, antimutagenic activity, and antiradical and antioxidant activities [14]. The cytotoxic effect of berberine depends on the type of cell line [12, 15]. DNA damage by berberine has been detected by a variety of methods [16].

The objective of this work was to investigate the effect of nanomaterials such as MWNT in DMF, MWNT in aqueous sodium dodecyl sulfate (SDS) solution, GNP, and a GNP–MWNT mixture in SDS, deposited on a carbon paste screen-printed electrode, on the response of the dsDNA electrochemical biosensor, by use of $[Co(phen)_3]^{3+}$, $K_3[Fe(CN)_6]$, and guanine moiety voltammetry. We report here the effect of the dispergation of MWNT with a surfactant, SDS. The hydrophobic chain of the surfactant can interact with the sidewall of the carbon nanotubes by hydrophobic interactions and thereby anchor the surfactant molecules on to the MWNTs, leaving hydrophilic head groups pointing into the solution [17]. The hydrophilicity of the head groups and their electrostatic properties essentially result in solubilization of the MWNT in aqueous medium. The non-covalent approach may be superior to covalent methods, because of its ability to maintain the electrical and structural properties of the MWNT [18]. The nanostructured DNA biosensor with the MWNT in SDS was used to study the effect of berberine on DNA isolated from human cancer cells (U937 cells) and non-cancer cells (keratinocytes).

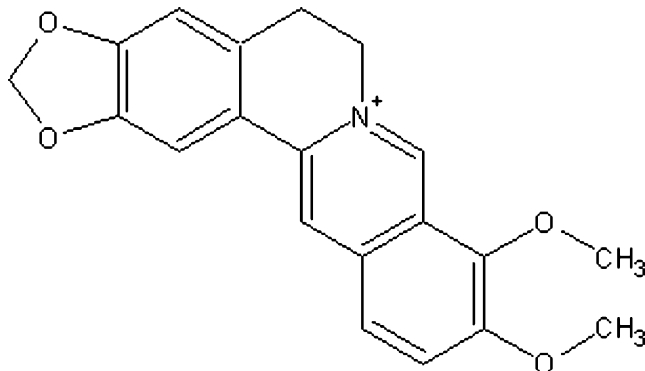


Fig. 1 Chemical formula of berberine

Experimental

Apparatus

An ECA pol, model 110 (Istran, Bratislava, Slovakia) computerized voltammetric analyzer fitted with a screen-printed three-electrode assembly (Food Research Institute, Bratislava, Slovakia) including a carbon working electrode (SPE, 25 mm² geometric surface area), a silver/silver chloride reference electrode (Ag/AgCl/SPE with a potential of 0.284 V relative to a conventional Ag/AgCl/sat. KCl electrode), and a counter electrode were used. Measurements were performed in a 10 mL glass one-compartment voltammetric cell at room temperature (22 °C).

Reagents

Multi walled carbon nanotubes (OD 40–60 nm, ID 5–10 nm, length 0.5–500 μm) were obtained from Aldrich. Their suspension was prepared in pure DMF from Lachema or in a 1% aqueous solution of SDS from Sigma. Colloidal gold nanoparticles (D 3.5–6.5 nm, 0.75 A₅₂₀ units mL⁻¹ PBS) were from Sigma.

Calf thymus dsDNA was obtained from Merck and used as received. Its stock solution (0.1 mg mL⁻¹) was prepared in 10 mmol L⁻¹ Tris-HCl and 1 mmol L⁻¹ EDTA solution of pH 8.0 and stored at -4 °C. The complex compound $[Co(phen)_3](ClO_4)_3$ was synthesized in our laboratory, as described elsewhere [19], and checked by chemical analysis. All other chemicals were of analyte-reagent-grade purity. Deionized and double distilled water was used throughout. PBS was 5 mmol L⁻¹ or 0.1 mol L⁻¹ concentration and pH 7.0.

The human promonocytic cell line U937 was from the American Type Culture Collection (Rockville, MD, USA). The human keratinocytes and U937 cells were cultivated in minimal Eagle medium (Biocom Bratislava).

Berberine (2,3-methylenedioxy-9,10-dimethoxyprotoberberine) from Sigma was dissolved in dimethyl sulfoxide (DMSO) from (Biocom, Bratislava) to furnish a stock solution of 7.5 mg mL⁻¹. Test solutions were prepared by adding appropriate amounts to 5 mmol L⁻¹ PBS; the final content of DMSO never exceeded 1%.

Isolation of DNA from cancer and non-cancer cells

U937 cells and keratinocyte cells (both 1×10^6) were harvested, washed with PBS, and then lysed in 100 μL solution (10 mmol L⁻¹ TRIS, 10 mmol L⁻¹ EDTA, 0.5% Triton X-100) supplemented with proteinase K (1 mg mL⁻¹). Samples were then incubated at 37 °C for 1 h and heated at 70 °C for 10 min. After lysis, RNA-ase (200 μg mL⁻¹) was added and incubation at 37 °C was repeated for 1 h [20]. The

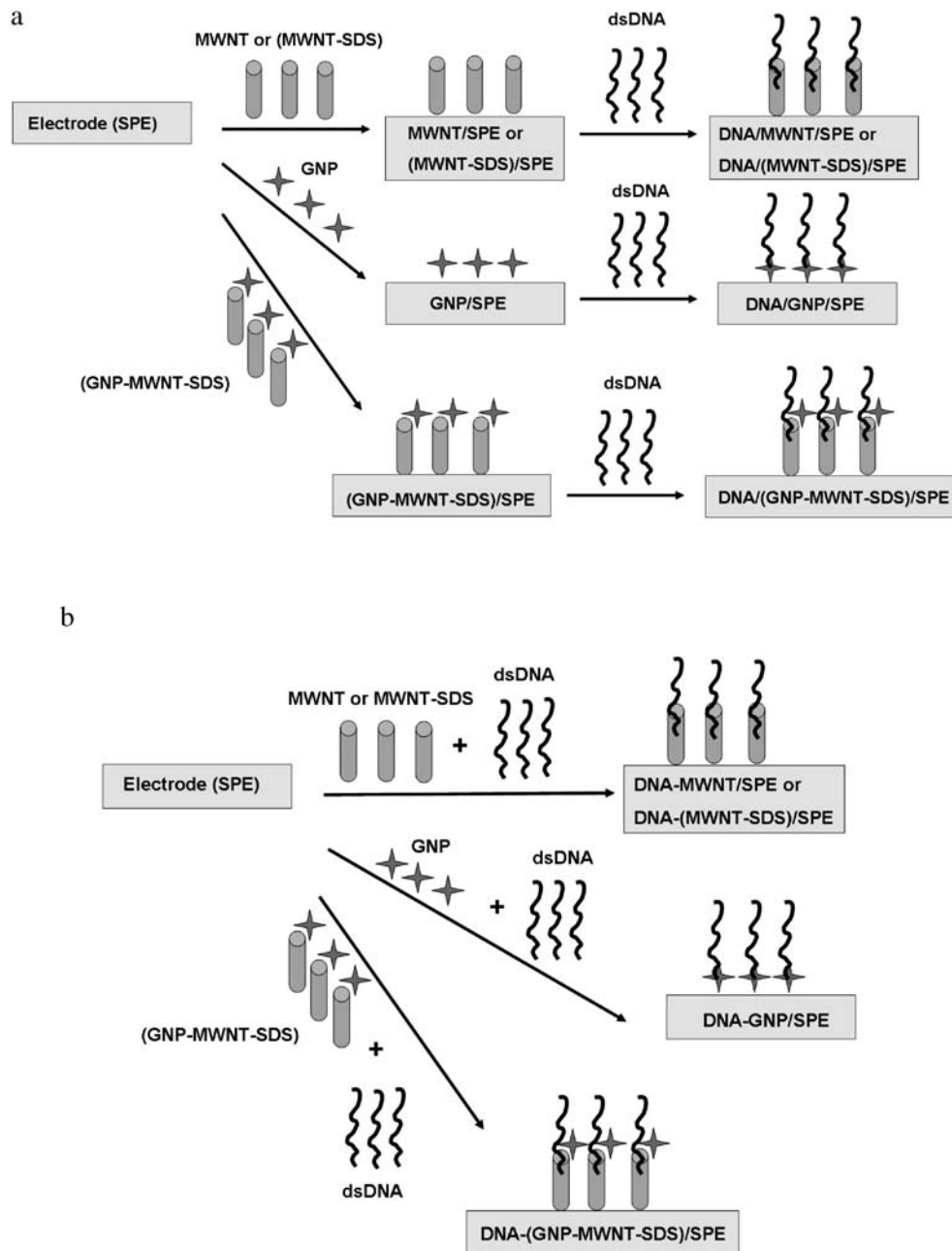
resulting mixture was used without other treatment. This mixture (5 µL) at room temperature was used for preparation of the DNA-modified electrodes as described below.

Preparation of modified electrodes

DNA/SPE

The DNA stock solution (0.1 mg mL⁻¹, 5 µL) was dropped on to the bare SPE surface and left to evaporate to dryness overnight. The nanostructured films were prepared by two ways (Fig. 2) layer-to-layer coverage (DNA/nanomaterial/SPE) and mixed coverage (DNA–nanomaterial/SPE).

Fig. 2 Schematic illustration of preparation of the nanostructured films: (a) layer-to-layer coverage (DNA/nanomaterial/SPE); (b) mixed coverage (DNA–nanomaterial/SPE)



DNA/nanomaterial/SPE

The MWNT suspensions (1 mg MWNT in 2 mL DMF or 1 mg MWNT in 2 mL 1% SDS; 5 µL), the GNP suspension (GNP in 5 mmol L⁻¹ PBS, 5 µL), or the GNP–MWNT suspension mixture (1:1 v/v GNP–MWNT in 1% SDS, 5 µL) were applied as drops to the bare SPE surface and left to evaporate to dryness. MWNT/SPE, (MWNT–SDS)/SPE, GNP/SPE, and (GNP–MWNT–SDS)/SPE were then modified by adding 5 µL of DNA stock solution (0.1 mg mL⁻¹) as a drop and evaporating overnight.

DNA-nanomaterial/SPE

The MWNT suspensions (1 mg MWNT in 2 mL DMF and 1 mg MWNT in 2 mL 1% SDS), the GNP suspension (GNP in 5 mmol L⁻¹ PBS) or the GNP–MWNT mixed suspension (1:1 v/v GNP–MWNT in 1% SDS, 5 µL) were mixed with the DNA stock solution (0.1 mg mL⁻¹) in the volume ratio 1:1. The resulting suspension (5 µL) was then applied as a drop to the bare SPE surface and left to evaporate to dryness.

Procedures

Differential pulse voltammetry of [Co(phen)₃]³⁺

Before the first measurement the DNA-modified electrode was immersed in 5 mmol L⁻¹ PBS, pH 7.0, for 5 min, with stirring. The procedure described elsewhere [21] was used. Briefly, the DNA marker [Co(phen)₃]³⁺ was accumulated from its 5 × 10⁻⁷ mol L⁻¹ solution in 5 mmol L⁻¹ PBS for 120 s at open circuit, with stirring. The cathodic DP voltammogram was recorded immediately from 200 to -400 mV at pulse amplitude 100 mV and scan rate 10 mV s⁻¹. The marker DPV peak current was evaluated against a baseline using the standard software and corrected to blank (I_0). The DNA-modified electrode was then regenerated by immersing the sensor in a solution of a high ionic strength (0.1 mol L⁻¹ PBS) for 120 s, with stirring, to remove accumulated [Co(phen)₃]³⁺ ions from the DNA layer. The marker peak current was found to be negligible when the DPV was performed on the blank solution.

To detect the effect of berberine on DNA, the same sensor was incubated in berberine solution (75, 50, 10, 1, or 0.1 µg mL⁻¹) in 5 mmol L⁻¹ phosphate buffer, pH 7.0, for 10 min, with stirring, and rinsed with water. The DNA marker peak current was obtained in duplicate. After the exchange of the medium for 5 × 10⁻⁷ mol L⁻¹ [Co(phen)₃]³⁺ in 5 mmol L⁻¹ PBS and accumulation of the marker, the mean value was calculated (I). Finally, the normalized (relative) signal I/I_0 was obtained.

Cyclic voltammetry of K₃Fe(CN)₆

Before the first measurement, the DNA-modified electrode was immersed in the 0.1 mol L⁻¹ PBS pH 7.0 for 5 min, with stirring. The cyclic voltammogram of 1 mmol L⁻¹ K₃Fe(CN)₆ in 0.1 mol L⁻¹ PBS was recorded from 600 to -400 mV using a scan rate of 50 mV s⁻¹ and evaluated against the CV record in blank PBS.

Differential pulse voltammetry of the guanine moiety

Before measurement the DNA-modified electrode was immersed in 5 × 10⁻³ mol L⁻¹ PBS, pH 7.0, for 5 min, with

stirring. The anodic DP voltammogram was immediately recorded in 5 mmol L⁻¹ blank PBS from 300 to 1100 mV with pulse amplitude 100 mV and scan rate 10 mV s⁻¹. The guanine peak current was evaluated against baseline. The procedure described elsewhere [22] was used.

Results and discussion

Electrochemical characteristics of the DNA marker [Co(phen)₃]³⁺

Table 1 shows current and potential data for the DP voltammetric signal of the reduction of [Co(phen)₃]³⁺ obtained at the prepared sensors. The current signal of the marker revealed modification of SPE with the mixture of DNA and nanomaterial (the mixed coverage, DNA–nanomaterial/SPE) is usually more effective than modification by use of the layer-to-layer technique (DNA/nanomaterial/SPE) for which signal enhancement is similar to that for simple DNA/SPE and SPE sensors. From Table 1 it can be seen that the highest marker signals were obtained for the DNA-GNP/SPE and DNA-(MWNT-SDS)/SPE biosensors. A combination of GNP and MWNT in SDS (GNP–MWNT nanohybrid) was, therefore, also tested. The marker signal obtained from the corresponding nanohybrid modified electrode, DNA-(GNP–MWNT-SDS)/SPE, was, however, approximately the same as those from the DNA-GNP/SPE and DNA-(MWNT-SDS)/SPE sensors. Hence, there is no synergism of the effects of the nanomaterials.

Table 1 Differential voltammetric peak current and peak potential obtained after accumulation of the marker Co[(phen)₃]³⁺ for 120 s from 5 × 10⁻⁷ mol L⁻¹ solution in 5 mmol L⁻¹ PBS, pH 7.0

Type of electrode	I_p (µA)	E_p (mV)	I_2/I_1 ^a
SPE	0.38	-100	—
DNA/SPE	1.46	-110	3.9
DMF/SPE	0.32	-102	—
MWNT/SPE	1.31	-132	—
DNA/MWNT/SPE	5.42	-132	4.1
DNA-MWNT/SPE	7.80	-140	5.9
GNP/SPE	0.31	-72	—
DNA/GNP/SPE	1.72	-72	5.5
DNA-GNP/SPE	2.12	-74	6.8
SDS/SPE	0.26	-98	—
(MWNT-SDS)/SPE	1.10	-94	—
DNA/(MWNT-SDS)/SPE	5.00	-94	4.5
DNA-(MWNT-SDS)/SPE	7.42	-130	6.7
(GNP–MWNT-SDS)/SPE	2.20	-94	—
DNA/(GNP–MWNT-SDS)/SPE	12.01	-104	5.4
DNA-(GNP–MWNT-SDS)/SPE	14.49	-124	6.6

^a I_2/I_1 is the ratio of the peak current for electrodes coated with DNA with nanomaterials (I_2) and with nanomaterials only (I_1)

DNA- $[Co(phen)_3]^{3+}$ dissociation rate constant

Dissociation of $[Co(phen)_3]^{3+}$ accumulated on the electrode surfaces was tested after transfer of the individual sensors into blank 5 mmol L⁻¹ PBS. The logarithm of the $[Co(phen)_3]^{3+}$ reduction peak current, I_p , depends linearly on the dissociation time, illustrating the first-order reaction kinetics. The values of dissociation rate constant (k) are summarized in Table 2. In general, the dissociation rate constants for mixed electrode coverage are smaller than those for layer-to-layer coverage. The strongest interaction of the $[Co(phen)_3]^{3+}$ complex with dsDNA, rate constant $5.5 \pm 0.1 \times 10^{-4} \text{ s}^{-1}$, was found for DNA-(MWNT-SDS)/SPE. The weakest interaction, rate constant $61.4 \pm 5.1 \times 10^{-4} \text{ s}^{-1}$, was at simple DNA/SPE.

These results are indicative of some differences between DNA structural arrangement and marker-binding ability at sensor surfaces with and without nanostructured materials. Stable marker binding is of great interest for the detection schemes using electrode transfer.

Cyclic voltammetry of K₃[Fe(CN)₆]

On the basis of the results obtained above, electrodes modified with a mixture of DNA and nanomaterials were chosen for testing with K₃[Fe(CN)₆] as redox indicator in the solution phase (Fig. 3). The function of this indicator is based on electrostatic repulsion of the Fe(CN)₆³⁻ anion and the negatively charged DNA phosphate backbone. From comparison of the curves 7 and 9 and of 3 and 5 it follows that an advantage of SDS for MWNT dispersion is significant despite its negative charge, which could be a barrier for the hexacyanoferrite anion. Evidently this because of the optimized amount of SDS used.

At the bare SPE, the CV of K₃[Fe(CN)₆] is characterized by the anodic to cathodic peak potential separation of 640 mV. When covered with DNA, the peak potential

Table 2 Rate constant for dissociation of the $[Co(phen)_3]^{3+}$ from the sensor surface, tested after transfer of the electrodes into blank 5 mmol L⁻¹ PBS. The complex was accumulated from its 5×10^{-7} mol L⁻¹ solution in 5 mmol L⁻¹ PBS for 120 s

Type of electrode	Dissociation rate constant, $k (\text{s}^{-1}) \times 10^4$
DNA/SPE	61.4 ± 5.1
DNA/MWNT/SPE	17.4 ± 0.9
DNA-MWNT/SPE	9.7 ± 0.8
DNA/GNP/SPE	54.5 ± 0.6
DNA-GNP/SPE	25.1 ± 0.4
DNA-(MWNT-SDS)/SPE	16.8 ± 0.6
DNA-(GNP-MWNT-SDS)/SPE	5.5 ± 0.1
DNA/(GNP-MWNT-SDS)/SPE	21.3 ± 1.7
DNA-(GNP-NT-SDS)/SPE	9.4 ± 0.7

separation was even worse, approximately 870 mV. Nano-materials improve the redox reversibility of hexacyanoferrite at both the electrodes, i.e. without and with DNA. The best results were obtained by use of (MWNT-SDS)/SPE ($\Delta E_p = 115$ mV) and DNA-(MWNT-SDS)/SPE ($\Delta E_p = 395$ mV) and by use of (GNP-MWNT-SDS)/SPE ($\Delta E_p = 115$ mV) and DNA-(GNP-MWNT-SDS)/SPE ($\Delta E_p = 465$ mV). Consequently, the difference between the CV profiles for these electrode couples enables detection of the presence and state of the DNA on the electrode surface. The ΔE_p values for curves 6 or 10 and the difference between the currents for curves 5 and 6 or for curves 9 and 10 measured at the K₃[Fe(CN)₆] cathodic peak potential at (GNP-MWNT-SDS)/SPE (curve 5) and (MWNT-SDS)/SPE (curve 9) were evaluated.

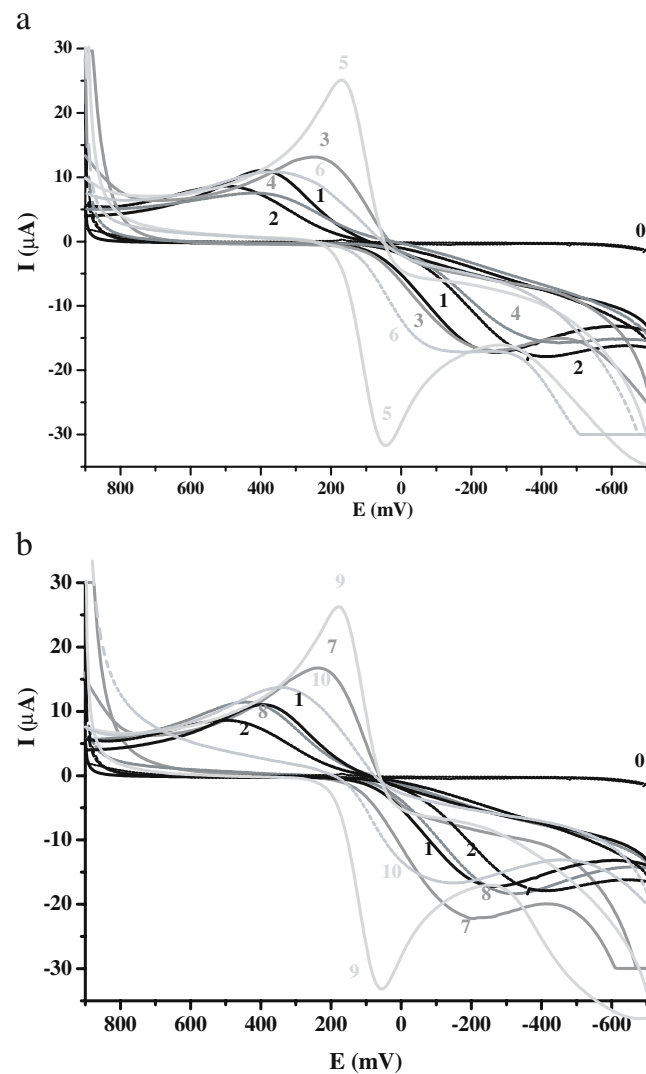


Fig. 3 CV scans of 1 mmol L⁻¹ K₃Fe(CN)₆ in 0.1 mol L⁻¹ PBS pH 7.0. The scan rate was 50 mV s⁻¹. (a) Blank (0), SPE (1), DNA/SPE (2), GNP/SPE (3), DNA-GNP/SPE (4), (GNP-MWNT-SDS)/SPE (5) and DNA-(GNP-MWNT-SDS)/SPE (6). (b) Blank (0), SPE (1), DNA/SPE (2), MWNT/SPE (7), DNA-MWNT/SPE (8), (MWNT-SDS)/SPE (9) and DNA-(MWNT-SDS)/SPE (10)

Electrochemical detection of guanine

The ability of nucleic acids to accept or donate electrons on interaction with electrodes was reported more than 40 years ago [23]. DNA bases undergo oxidation at carbon electrodes. Guanine and adenine are oxidized in sequence of $2e^- - 2H^+$ steps to give 8-oxoguanine and 2-oxyadenine and 2,8-dioxyadenine which are transformed further in follow-up reactions [24]. Current signals of guanine and adenine oxidation differ according to number of the electrooxidation steps.

The voltammetric signal for oxidation of the DNA guanine and DNA adenine residues at nanomaterial modified electrodes DNA-GNP/SPE, DNA-MWNT/SPE, DNA-(MWNT-SDS)/SPE and DNA-(GNP-MWNT-SDS)/SPE was investigated and compared with that obtained at the simple DNA/SPE electrode (Fig. 4). The nanomaterials MWNT in DMF or SDS and the GNP–MWNT nanohybrid cause a negative potential shift of the DPV signal of the guanine moiety from 840 mV for DNA/SPE to 685 mV, 690 mV and 690 mV for DNA-MWNT/SPE, DNA-(MWNT-SDS)/SPE, and DNA-(GNP-MWNT-SDS)/SPE, respectively, without any significant change in the value of the current. Similarly, the negative shift of oxidation of the adenine moiety from 1290 mV (at DNA/SPE) to 1067 mV, 1064 mV, and 1091 mV (for DNA-MWNT/SPE, DNA-(MWNT-SDS)/SPE and DNA-(GNP-MWNT-SDS)/SPE, respectively) can be seen in Fig. 4. The negative shift of potential for oxidation of the DNA bases observed for MWNT-modified electrodes can be ascribed to the electrocatalytic properties of MWNT and, consequently, reduction of the energy of the process. A similar shift has been reported for other analytes with poor electrochemical

behaviour, for example ascorbic acid and dopamine [25, 26].

To confirm the results, 1×10^{-5} mol L⁻¹ guanine solution in PBS was tested as the standard. The DPV guanine signal for the SPE was found to be 815 mV and that for the (MWNT-SDS)/SPE was 610 mV. Hence, because of the electrocatalytic properties of the nano-materials used the indicator-less and mediator-less detection schemes with these biosensors can be considered for evaluation of changes in DNA structure and in the redox state of DNA bases.

The effect of berberine

DNA-(MWNT-SDS)/SPE sensors with DNA obtained from cells were fabricated using the general biosensor preparation procedure given in the experimental section. In studies of the effect of berberine the amount of DNA applied to the electrode surface was again tested by monitoring the DPV signal of the $[Co(phen)_3]^{3+}$ complex as the DNA redox marker. Because this signal was almost the same for both the sensor with DNA isolated from U937 cells and that with DNA from keratinocytes, in the berberine studies the starting value of the absolute marker signal for DNA both from U937 cells and from keratinocytes was the same.

Normal and cancer cells can, however, differ in the amount and type of DNA. In general, loss of control over cell division, characteristic of cancer, can result in tumour cells with abnormal amounts of DNA. The predominant theory of cancer is that changes of components within the DNA molecule (mutation of some types of gene) lead to the development of cancer [27]. The secondary structure of DNA in cancer cells differs from normal DNA in that it contains some permanently open loops [28]. These permanently separated sections allowed more substances to come between the two strands of the double helix. Le Goff et al. [29] referred to cancerous DNA as destabilized DNA, because the hydrogen bonds did not hold the two strands together in a stable manner.

Before the berberine investigation, we checked the stability of the human DNA on the sensor surface. After 5 min pretreatment in blank 5 mmol L⁻¹ PBS pH 7.0 solution with stirring, the final DNA marker signal is rather stable and can be exploited analytically with sufficient repeatability (the RSD of the $[Co(phen)_3]^{3+}$ signal was 11% for DNA from U937 cells and 12% for DNA from keratinocytes, $n=7$). This confirms the stability of DNA immobilization and indicates also that potential impurities present in the DNA layer have no significant effect on the measurements.

The effect of berberine on DNA was evaluated by using the voltammetric techniques described above after an incubation of the biosensor in solutions of berberine at

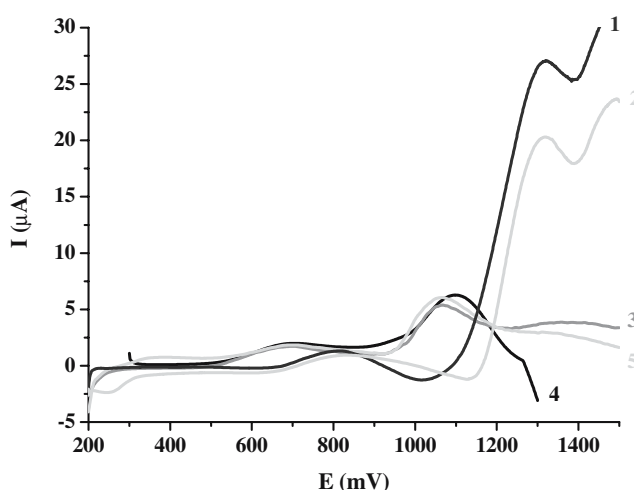


Fig. 4 DP voltammograms obtained from the DNA guanine and adenine moieties. Working electrodes: DNA/SPE (1), DNA-GNP/SPE (2), DNA-MWNT/SPE (3), DNA-(MWNT-SDS)/SPE (4) and DNA-(GNP-MWNT-SDS)/SPE (5). Conditions: 5 mmol L⁻¹ PBS, pH 7.0, scan rate 10 mV s⁻¹, pulse amplitude 100 mV

concentrations in the range 0.1 to 75 $\mu\text{g mL}^{-1}$. A berberine concentration-dependent change (probably damage) to DNA from both cancer and non-cancer cells attached to the electrode surface was found. This is indicated by a decrease in the relative $[\text{Co}(\text{phen})_3]^{3+}$ signal (I/I_0), which represents the portion of dsDNA which survives incubation in the berberine solution (Fig. 5).

The manner in which berberine interacts with DNA, by intercalation, has been reported previously [30–33]. In low ionic strength solution berberine forms an intercalation complex with dsDNA [34]. Recent studies have shown that berberine intercalates into AATT-containing rather than GGCC-containing dsDNA [35, 36]. Thermodynamic data for the binding reaction may be divided into three contributions:

- the contribution from the molecular interactions between the bound ligand and the nucleic acid binding site as a result of hydrogen bonding and hydrophobic interactions;
- contributions arising from conformational changes in either the nucleic acids or the drug on binding; and
- contributions, for example ion release, proton transfer, or changes in the water of hydration which may be coupled with the other two processes [37].

Other studies have reported that the berberine molecule is located in the minor groove of the double helix of the oligonucleotide [38].

According to the literature, berberine can induce morphological changes and DNA fragmentation [39, 40]. It seems that interaction of berberine with DNA immobilized on the surface of our electrodes can also lead to strand breaks, double helix opening, and, finally, to fragmentation of the attached DNA. Small fragments of DNA can leach into the PBS solution, the amount of original DNA on the

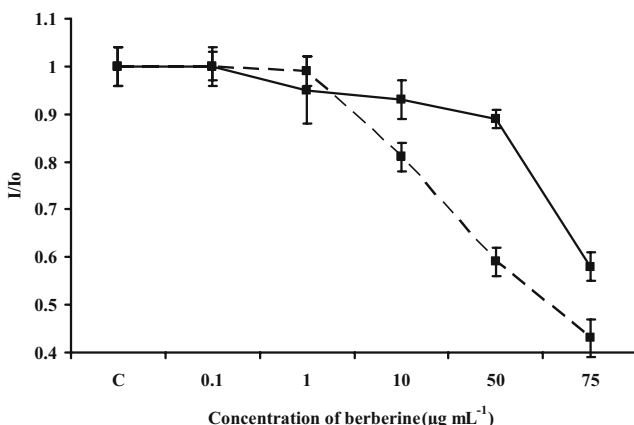


Fig. 5 Dependence of the relative marker signal ($n=3$) at the DNA-(MWNT-SDS)/SPE on the concentration of berberine. Sensors prepared with DNA from U937 cells (dashed line) and keratinocytes (unbroken line) were incubated in a solution of berberine in 5 mmol L^{-1} PBS for 10 min. C is control without berberine

electrode surface becomes smaller, and, consequently, the DNA marker signal diminishes. There is a difference in DNA sensor behaviour DNA from U937 cells is more sensitive to berberine than that from keratinocytes (Fig. 5). Separate tests with dsDNA from calf thymus have shown it to be even more stable toward berberine than DNA from keratinocytes. This can be explained by above mentioned structural instability of cancer DNA and specific interactions of berberine with DNA.

By use of CV of $\text{K}_3\text{Fe}(\text{CN})_6$, changes to DNA were again found to increase with increasing berberine concentration (Fig. 6) and the changes were, again, greater for DNA from cancer cells than for that from keratinocytes. The $\text{K}_3\text{Fe}(\text{CN})_6$ current (I_c) at the DNA-(MWNT-SDS)/SPE was measured at the potential corresponding to the CV cathodic peak of $[\text{K}_3\text{Fe}(\text{CN})_6]$ recorded at the MWNT-SDS/SPE electrode (+57 mV).

Incubation of the DNA-(MWNT-SDS)/SPE sensor in berberine also affected the DPV signal of the guanine and

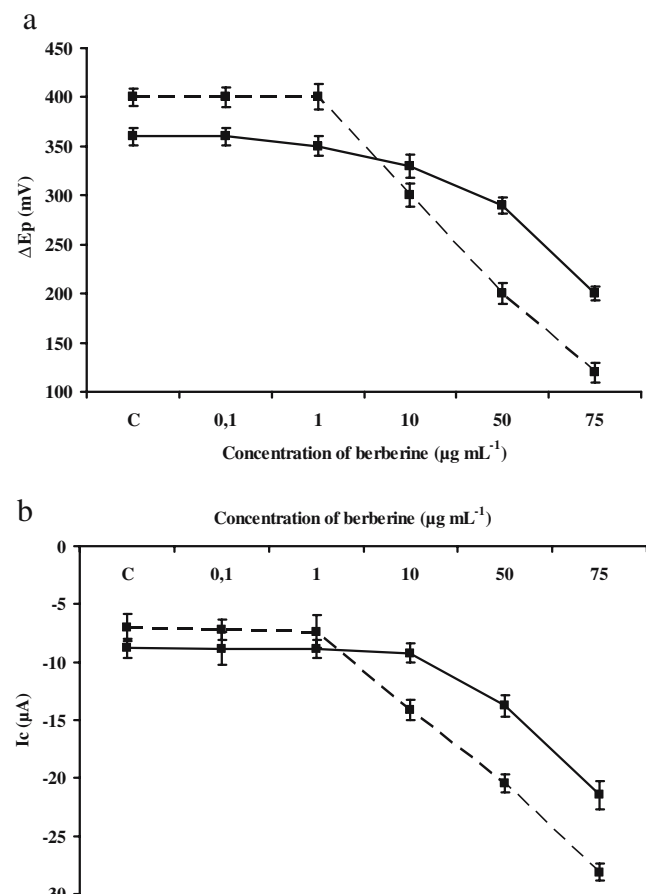


Fig. 6 Dependence on berberine concentration of the $\text{K}_3\text{Fe}(\text{CN})_6$ CV peak potential separation (a) and the cathodic peak current measured at 57 mV (b) obtained at a DNA-(MWNT-SDS)/SPE. Sensors with DNA from U937 cells (dashed line) and keratinocytes (unbroken line) were first incubated in a solution of berberine in 5 mmol L^{-1} PBS for 10 min, with stirring. C is control without berberine. Conditions: 1 mol L^{-1} $\text{K}_3\text{Fe}(\text{CN})_6$ in 0.1 mol L^{-1} PBS, pH 7.0, scan rate 50 mV s^{-1}

adenine moieties. Low concentrations of berberine (0.1 and 1 $\mu\text{g mL}^{-1}$), have no effect on the signals from DNA from U937 cells (3.0 μA for guanine and 10.1 μA for adenine) or from keratinocytes (2.0 μA for guanine moiety and 9.1 μA for adenine moiety). When the berberine concentration was 75 $\mu\text{g mL}^{-1}$, however, the guanine signals were of 0.7 μA and 1.2 μA and the adenine signals were 5.4 μA and 6.1 μA for U937 cells and keratinocytes, respectively, confirming the greater effect of berberine on DNA from the cancer cells.

Conclusions

The combination of MWNT nanostructures with dsDNA macromolecules is of great importance because leads to novel bioanalytical applications. Our experiments have revealed significant enhancement of the DNA marker signal and of DNA-[$\text{Co}(\text{phen})_3^{3+}$] binding stability. The voltammetric response for hexacyanoferrite, used as the indicator in solution, and that of guanine moiety were also significantly improved. Compared with DMF as medium for MWNT dispergation, with a risk of DNA denaturation at long contact times, the noncovalent functionalization of MWNT with surfactant (SDS) results in high solubility of MWNT in the aqueous medium and, evidently, distribution of electronic charge on the tubes' surface which mediates attachment of GNP to the MWNT. Compared with simple MWNT and GNP, however, use of the GNP–MWNT nanohybrid did not lead to a significant change in biosensor properties.

The anticancer agent berberine has an evident effect on DNA which depends on berberine concentration. DNA from normal keratinocytes was structurally much more stable toward the action of berberine than DNA from U937 cancer cells. It was demonstrated that the DNA-based biosensor acts as an effective chemical toxicity sensor which can be used for simple, rapid detection of DNA-damaging species and screening of DNA anticancer agents, for example berberine.

Acknowledgements This work was supported by the Research and Development Assistance Agency under contract No. APVT-20-015904.

References

- Zhao Q, Gan Z, Zhuang Q (2002) *Electroanalysis* 14:1609–1613
- Labuda J, Fojta M, Jelen F, Paleček E (2006) In: Grimes CA, Dickey EC, Pishko MN(eds) *Encyclopedia of sensors*, vol 3. American Scientific Publishers, CA, USA, pp 201–228
- Avouris P (2002) *Chem Phys* 281:429–445
- Ferancová A, Ovádeková R, Vaníčková M, Šatka A, Viglaský R, Zima J, Barek J, Labuda J (2006) *Electroanalysis* 18:163–168
- Ellis AV, Vijayamohan K, Goswami R, Chakrapani N, Ramanathan LS, Ajayan PM, Ramanath G (2003) *Nano Lett* 3:279–282
- Tsai YCh, Chen JM, Li SC, Marken F (2004) *Electrochim Commun* 6:917–922
- Zhang M, Su L, Mao L (2006) *Carbon* 44:276–283
- Luo XL, Xu JJ, Wang JL, Chen HY (2005) *Chem Commun* 16:2169–2171
- Cai H, Xu Ch, He P, Fang Y (2001) *J Electroanal Chem* 510:78–85
- Creasy WA (1979) *Biochem Pharmacol* 28:1081–1084
- Amin AH, Subbaiah TV, Abbasi KM (1969) *Can J Microbiol* 15:1067–1076
- Jantová S, Čipák L, Čerňáková M, Košťálová D (2003) *J Pharm Pharmacol* 55:1143–1149
- Kuo CL, Chi CW, Liu TY (2004) *Cancer Lett* 2:127–137
- Račková L, Mjeková M, Košťálová D, Štefek M (2004) *Bioorg Med Chem* 12:4709–4715
- Letašiová S, Jantová S, Mikó M, Ovádeková R, Horváthová M (2006) *J Pharm Pharmacol* 58:263–270
- Mazzini S, Bellucci MC, Mondelli R (2003) *Bioorg Med Chem Lett* 4:505–514
- Assael MJ, Chen CF, Metaxa I, Wakeham WAI (2004) *Int J Thermophys* 25:971–985
- Fu K, Huang W, Lin Y, Zhang D, Hanks TW, Rao AM, Suna YP (2002) *J Nanosci Nanotechnol* 2:457–461
- Dollimore LS, Gillard RD (1973) *J Chem Soc* 78:933–940
- Jantová S, Letašiová S, Repický A, Ovádeková R, Lakatoš B (2005) *Cell Biochem Function* (in press)
- Bučková M, Labuda J, Šandula J, Križková L, Štepánek I, Ďuračková Z (2002) *Talanta* 56:937–947
- Ovádeková R, Jantová S, Labuda J (2005) *Anal Lett* 38:2625–2638
- Paleček E (1958) *Naturwissenschaften* 45:186–187
- Vetterl V, Hasoň S (2005) In: Paleček E, Scheller F, Wang J (eds) *Electrochemistry of nucleic acids and proteins*, vol. 1. Elsevier, pp 51–57
- Rubianes MD, Rivas GA (2003) *Electrochim Commun* 5:689–694
- Valentini F, Orlanducci S, Terranova ML, Amine A, Palleschi G (2004) *Sens Actuators B* 100:117–125
- Beljanski M, Dutta SK (1987) *Oncology* 44:327–330
- Beljanski M, Crochet S (1996) *Int J Oncol* 8:1143–1148
- Le Goff L, Wicker M, Beljanski M (1988) *Med Sci Res* 16:359–361
- Barreto MC, Pinto RE, Arrabaça JD, Pavão ML (2003) *Toxicol Lett* 146:37–47
- Schmeller T, Latz-Brüning B, Wink M (1997) *Phytochemistry* 44:257–266
- Cushman M, Dekow FW, Jacobsen LB (1979) *J Med Chem* 22:331–333
- Krishnan P, Bastow KF (2000) *Anticancer Drug Des* 15:255–264
- Kluza J, Baldeyrou B, Colson P, Rasoanaivo P, Mambu L, Frappier F, Bailly Ch (2003) *Eur J Pharm Sci* 20:383–391
- Chen WH, Qin Y, Cai ZW, Chan CL, Luo GA, Jiang ZH (2005) *Bioorg Med Chem* 13:1859–1866
- Wu JF, Chen LX, Luo GA, Liu YS, Wang YM, Jiang ZH (2006) *J Chromatogr B* 833:158–164
- Yadav RCh, Kumar GS, Bhadra K, Giri P, Sinha R, Pal S, Maiti M (2005) *Bioorg Med Chem* 13:165–174
- Mazzini S, Bellucci MC, Mondelli R (2003) *Bioorg Med Chem* 11:505–514
- Kuo ChL, Chou CC, Yung BY (1995) *Cancer Lett* 93:193–200
- Miura N, Yamamoto M, Ueki T, Kitani T, Fukuda K, Komatsu Y (1997) *Biochem Pharm* 53:1315–1322